Theor Appl Climatol (2013) 112:29–43
DOI 10.1007/s00704-012-0699-6

ORIGINAL PAPER

Impact of freshwater discharge from the Greenland ice sheet on North Atlantic climate variability

Soon-Il An · Hyerim Kim · Baek-Min Kim

Received: 24 January 2012 / Accepted: 21 June 2012 / Published online: 18 July 2012

Abstract Using a coupled ocean–atmosphere general circulation model, we investigated the impact of Greenland ice sheet melting on North Atlantic climate variability. The positive-degree day (PDD) method was incorporated into the model to control continental ice melting (PDD run). Models with and without the PDD method produce a realistic pattern of North Atlantic sea surface temperature (SST) variability that fluctuates from decadal to multidecadal periods. However, the interdecadal variability in PDD run is significantly dominated in the longer time scale compared to that in the run without PDD method. The main oscillatory feature in these experiments likely resembles the density-driven oscillatory mode. A reduction in the ocean density over the subpolar Atlantic results in suppression of the Atlantic Meridional Overturning Circulation (AMOC), leading to a cold SST due to a weakening of northward heat transport. The decreased surface evaporation associated with the cold SST further reduces the ocean density and thus, simultaneously acts as a positive feedback mechanism. The southward meridional current associated with the suppressed AMOC causes a positive tendency in the ocean density through density advection, which accounts for the phase transition of this oscillatory mode. The Greenland ice melting process reduces the mean meridional current and meridional density gradient because of additional fresh water flux, which suppress the delayed negative feedback due to meridional density advection. As a result, the oscillation period becomes longer and the transition is more delayed.

S.-I. An (✉) · H. Kim
Department of Atmospheric Sciences, Yonsei University,
Seoul 120-749, South Korea
e-mail: sian@yonsei.ac.kr

B.-M. Kim
Korea Polar Research Institute, KORDI,
Incheon, South Korea

1 Introduction

The increased concentration of greenhouse gasses in the atmosphere has led to warmer climates during the twentieth century (IPCC 2007). The observed global warming signal was estimated to be about 0.6° over the last 100 years. However, the change in the surface temperature shows a distinct regional distribution. In particular, the recent surface temperature trend that appeared in observations and simulations by coupled general circulation models under the future climate scenario was consistent with so-called polar amplification (Holland and Bitz 2003; ACIA 2005; IPCC 2007), indicating that the Arctic region is the most vulnerable location to global warming. Evidently, the record for the smallest area of arctic sea ice has frequently been broken over the last few decades (Serreze et al. 2003; Rothrock et al. 2008), and the melting rate of continental ice sheets (such as the Greenland ice sheet), as observed from space and in the field, has continuously increased (Chen et al. 2006; there is also a regional difference in Greenland; Abdalati and Steffen 2001). Nevertheless, ocean reanalysis data obtained over the last 100 years (Deser et al. 2010) and coupled general circulation model simulations (Ting et al. 2009) have shown a negative sea surface temperature (SST) trend over the North Atlantic between 50–60° N. The mechanism for this negative trend has yet to be investigated, but it is presumably due to a slowing down of the Atlantic Meridional Overturning Circulation (AMOC) that has actually been observed in recent decades (Bryden et al. 2005). Furthermore, such change in Atlantic Ocean due to the greenhouse warming eventually modifies either climate state in terms of the long-term trend or climate variability in terms of the short-term decadal-to-multi-decadal variation. Thus, the continuous modification of climate variability is expected through the impact of long-term trend, and its possible mechanism needs to be revealed.

The AMOC is a major branch of the thermohaline circulation; its intensity depends on the salinity of the ocean and temperature changes. The ocean salinity is influenced by local precipitation, evaporation, and river runoff. Freshwater discharge from Greenland ice sheet melting also modifies the oceanic salinity. Therefore, global warming would sequentially lead to Greenland ice sheet melting, a reduction in oceanic salinity, a slowing down of the AMOC, a reduction in northward thermal transport, and a cooling trend over the North Atlantic. In contrast, cooling over the subpolar North Atlantic influences the surrounding atmosphere (Deser and Blackmon 1995; Kushnir 1994; Wohlleben and Weaver 1995) and presumably reduces the Greenland ice sheet-melting rate. Such an air–sea–ice feedback process exists in nature, but has yet to be fully investigated (Grossmann and Klotzbach 2009), in particular a possible modification of the climate variability associated with the change in the climate state.

In this work, a coupled general circulation model was used to examine the impact of Greenland ice sheet melting on North Atlantic climate variability spanning the interannual to interdecadal time scale. The reason for focusing on such temporal periods is that the dominant mode of North Atlantic climate variability is known to have a decadal-to-multidecadal time scale (Schlesinger and Ramankutty 1994; Eden and Jung 2001; Alvarez-Garcia et al. 2008). In addition, related physical processes such as ice melting, oceanic adjustment, AMOC changes, and local air–sea interactions must be identified as timescale response components for longer than one year. To examine the role of the Greenland ice sheet, we have parameterized the ice sheet-melting rate in the developed model as a function of the surface air temperature. Basically, we compared the results of two simulations conducted with and without ice sheet melting parameterization, and addressed how Greenland ice sheet melting affects North Atlantic climate variability.

In Section 2, the model and parameterization method are introduced. North Atlantic climate oscillation features simulated by the coupled model and a possible mechanism of the oscillation are detailed in Section 3. The role of Greenland ice sheet melting is presented in Section 4. Conclusions are ultimately given in Section 5.

2 Model, parameterization, and experimental designs

2.1 Fast ocean atmosphere model

The Fast Ocean Atmosphere Model (FOAM) was developed jointly at the University of Wisconsin-Madison and Argonne National Laboratory (Jacob 2007). The atmospheric model is a parallel version of the National Center for Atmospheric Research Community Climate Model version 2 (CCM2), but the atmospheric physics were replaced by those from CCM3. The ocean model was developed from the Geophysical Fluid Dynamics Laboratory Modular Ocean Model. The FOAM used in this work has an atmospheric resolution of R15 with 18 vertical layers in a hybrid sigma pressure coordinate system, and an oceanic resolution of 1.4° latitude by 2.8° longitude with 24 vertical levels. The model also includes a thermodynamic sea ice model. The FOAM captures most major features of the observed climate, including the El Nino-Southern Oscillation (Liu et als. 2000), Atlantic climate variability (Wu and Liu 2002, 2005), Pacific decadal variability (Wu et al. 2003), etc. More information can be found at http://www.mcs.anl.gov/research/projects/foam/index.html.

2.2 Positive degree-day method

To compute the melting rate of the Greenland ice sheet, the positive degree-day (PDD) method was incorporated into the FOAM. The PDD method is a parameterization of the melting rate of snow and ice at the surface of an ice sheet or glacier. It is a simple, empirical relation that states that the melting rate is proportional to surface-air temperatures above 0 °C (Braithwaite and Olesen 1989; Hock 2003). The physical basis of this method and its related temperature-based melt index methods were examined by Braithwaite (1995) and are used in this study. The PDD model here is basically same as in Braithwaite (1995), and thus the total ablation A over an N day period is given by:

$$A = \alpha \sum_{t=1}^{t=N} H_t + \beta \sum_{t=1}^{t=N} H_t T_t \tag{1}$$

where H_t=1.0 when T_t>0 °C and H_t=0.0 when T_t<0 °C; the parameters α and β represent the melting with an air temperature of 0 °C and the increase of ablation with temperature, respectively. The first and second summations indicate the number of days (N*) with temperatures at or above the melting point, and the PDD sum for the N day period. Therefore, the daily mean ablation rate for the N day period (A/N) becomes $\alpha(N^*/N)+\beta(\mathrm{PDD}/N)$. In this study, α is a constant of 3 mm day^{-1}, and β for the air temperature T_{mj} is following;

$$\begin{aligned}
&\text{For South of } 72^\circ\,\text{N}\\
&\beta_{\mathrm{ice}} = \beta^{w}_{\mathrm{ice}}\\
&\text{For North of } 72^\circ\,\text{N}\\
&\beta_{\mathrm{ice}} = \begin{cases} \beta^{w}_{\mathrm{ice}} & T_{\mathrm{mj}} \geq T_w, \\ \beta^{w}_{\mathrm{ice}} + \frac{\beta^{c}_{\mathrm{ice}} - \beta^{w}_{\mathrm{ice}}}{(T_w - T_c)^3}\left(T_w - T_{\mathrm{mj}}\right)^3 & T_c \leq T_{\mathrm{mj}} \leq T_w, \\ \beta^{c}_{\mathrm{ice}} & T_{\mathrm{mj}} \leq T_c. \end{cases}\\
&T_w = 10\,^\circ\mathrm{C},\quad T_c = -1\,^\circ\mathrm{C},\\
&\beta^{w}_{\mathrm{ice}} = 7\,\mathrm{mm}\ d^{-1}\,^\circ\mathrm{C}^{-1}\ \text{and}\ \beta^{c}_{ice} = 15\,\mathrm{mm}\ d^{-1}\,^\circ\mathrm{C}^{-1}
\end{aligned} \tag{2}$$

The PDD method is different from an active ice sheet model such that the growth of ice sheet is not accounted but the ablation does. Nevertheless, since we set up the

complete melting of snow cover as a precondition for the ice sheet melting, to some extent both accumulation and melting of ice sheet are taken into account in this model.

2.3 Experimental design

Without flux adjustment, fully coupled control simulations (CTL) have been performed over a time scale of 1,000 years; no apparent climate drifts have been observed (not shown here). Such a long-term simulation is necessary to account for the spin-up of the ocean. Data from the past year are used as an initial condition for each experiment. Here, we perform two experiments: one for the "CTL-run" without PDD parameterization and another for the "PDD-run" with PDD parameterization. Each run was integrated for 500 years and the last 200-year results were subsequently analyzed.

3 Mean climate states

Climate state changes caused by Greenland ice sheet melting are identified as the difference between the total mean for the PDD run and that for the CTL run. Here, the mean indicates the average over the last 200 years of each run. The SST, salinity, meridional stream function of the ocean (a measure of the intensity of the AMOC), and P–E data (precipitation minus evaporation at the surface) are shown in Fig. 1. As evident in Fig. 1a, a negative SST with a maximum of about −1.0 °C centered at 50° N, 45° W is observed over the subpolar North Atlantic. In the same region, a negative surface air temperature with a maximum of −2 °C was also observed (not shown). Negative salinity appears in the Baffin Bay and Labrador Sea. This negative salinity spreads down to the subpolar North Atlantic, where the negative SST region is located (Fig. 1b). The decreased salinity in the PDD run is obviously related to the freshwater discharge of the melted Greenland ice sheet. The mean freshwater discharge in the PDD run was about 0.0116 Sv higher than that in the CTL run (see Fig. 10). The density difference pattern is almost identical to the salinity pattern (not shown) and thus, the negative density region is somewhat collocated over the negative SST area. This indicates that density changes mainly follow salinity changes, but not temperature changes. The lower density obviously leads to a slowing down of the AMOC (Fig. 1c) and thus, northward heat transport is reduced (Dickson and Brown 1994; Marshall and Schott 1999) and the North Atlantic SST is decreased, as seen in Fig. 1a. Interestingly, the cooling and freshening of the subpolar North Atlantic and the slowing down of the AMOC in the PDD run are consistent with recently observed trends (Bryden et al. 2005; Deser et al. 2010; Lozier et al. 2010). Furthermore, a positive surface freshwater flux (P–E) is observed over the negative density (salinity) region (Fig. 1d), which should cause a further decrease in the density. The increase in the P–E is mainly due to a decrease in surface

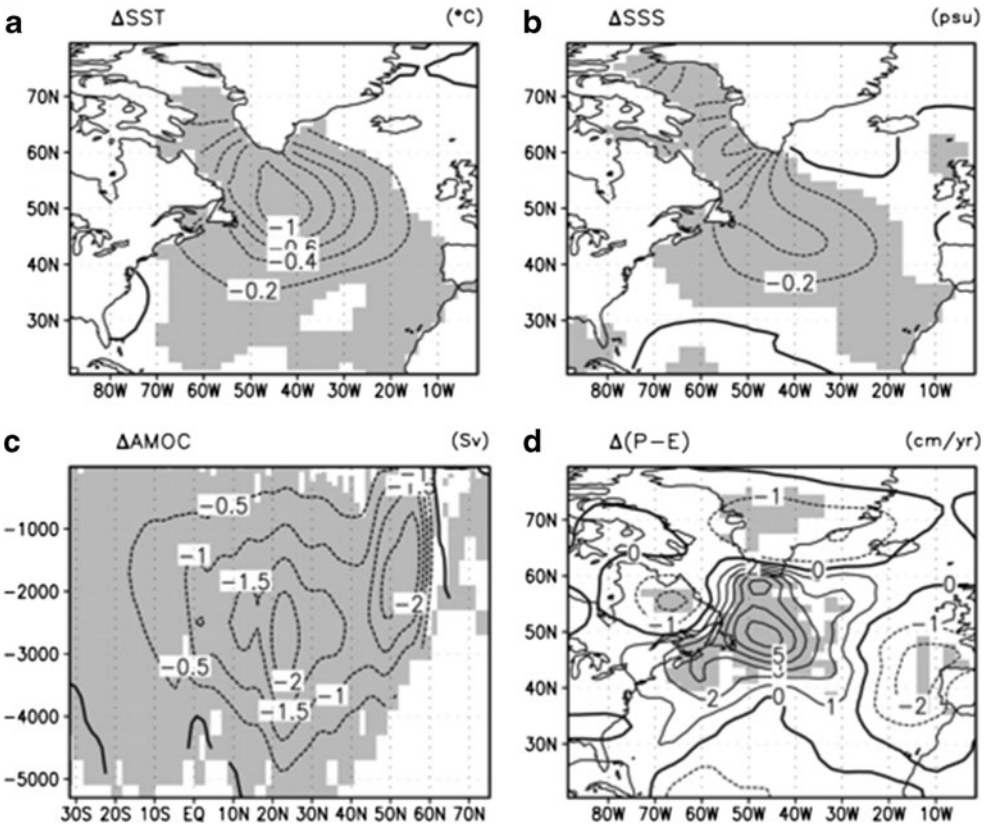

Fig. 1 Differences (PDD minus CTL) in the mean **a** SST, **b** salinity, **c** meridional stream function, and **d** P–E for the PDD run and CTL run. The mean indicates the temporal average for the last 200 years. Units for the SST, salinity, meridional stream function, and P–E are degree Celcius, practical salinity unit, sverdrups, and centimeter per year, respectively. *Shading* indicates the statistically significant region with 95 % confidence tested by *t* test. Contour intervals in the SST, salinity, stream function, and P–E are 0.2, 0.2, 0.5, and 1, respectively

evaporation caused by the cold SST rather than an increase in precipitation, and it may be also due to the associated atmospheric circulation (not shown here). Through the aforementioned processes, a positive feedback loop to cool the mean SST over the North Atlantic was obtained. However, it is also expected that SST cooling contributes to a cold surface air temperature, which in turn prevents further melting of the ice sheet. Consequently, the mean SST over the North Atlantic Ocean is sustained.

4 Climate variability

To identify the dominant mode of climate variability over the North Atlantic, principal component analysis (PCA, also known as empirical orthogonal function analysis (EOF)) was applied to the observed and simulated North Atlantic SSTs. Here, the observed SST was obtained from the National Oceanic and Atmospheric Administration Extended Reconstructed SST version 3 dataset, which spans almost 100 years from 1900 to the present (Smith et al. 2008). To remove intraseasonal variation, the annual average with a center of the boreal winter was taken before applying PCA. As shown in Fig. 2a, the first PCA mode of the observed North Atlantic SST anomalies shows a monopole pattern (also referred to as the North Atlantic monopole by Wu and Liu (2005)) with a center located at 40°W, 55°N. Overall, the major temporal fluctuations obtained from the spectrum analysis of the principal components (PC) of this first PCA mode show a broad spectrum with dominant peaks around 50 years and slightly less than 10 years. The leading SST modes obtained from both the CTL and PDD runs are similar to those derived from observations, but the variance explained by the first PCA mode from the model (60.5 % for the CTL run and 65.9 % for the PDD run) is larger than that from observations (40.0 %). The broad spectral density distributions from both runs are similar to those from observations. However, significant peaks around 10–20 years are observed in the CTL run, while those for the PDD run are around 15–30 years. Such findings indicate that Greenland ice melting seems to lengthen the main period of North Atlantic climate variability. The slow time scale variation will be discussed in Section 5. On the whole, both the CTL and PDD runs simulate the dominant mode of the North Atlantic SST reasonably well.

4.1 Wind driven

To identify the atmospheric pattern associated with the first PCA mode, the lagged regressions of 500 hPa geopotential height anomalies against the PC of the first PCA were computed for the CTL and PDD runs. To isolate the

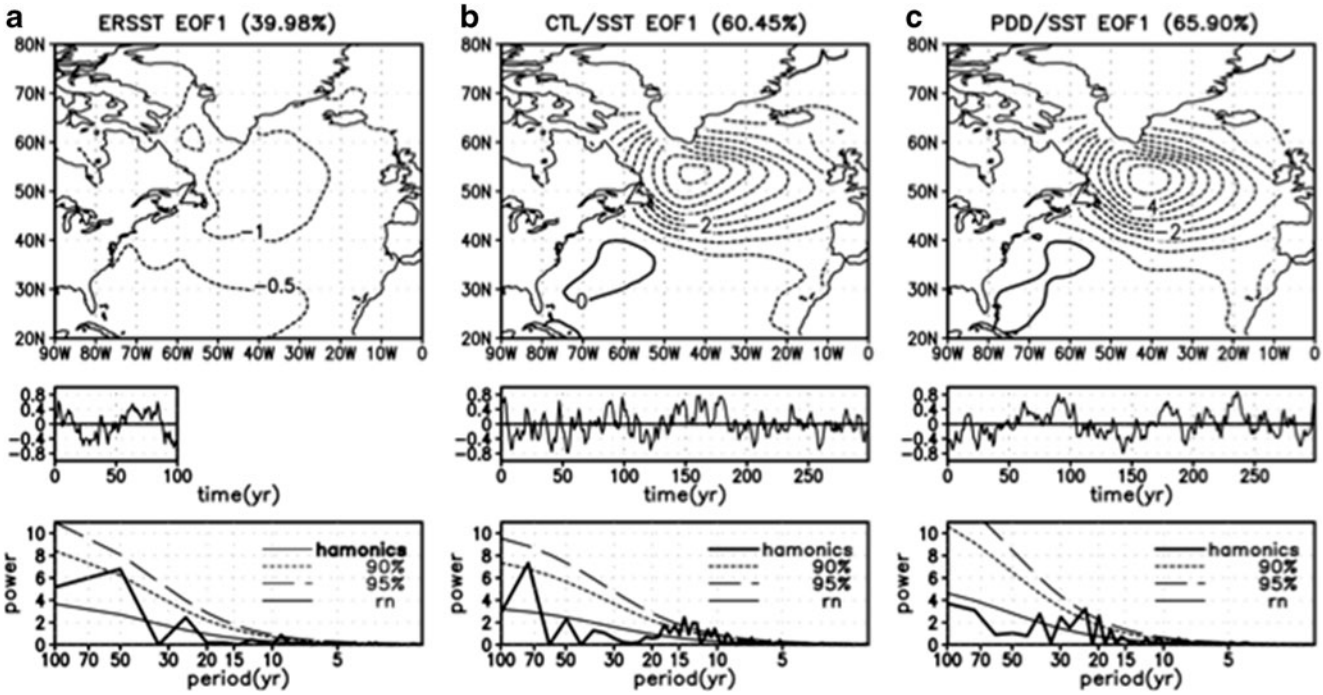

Fig. 2 **a** First PCA mode of the North Atlantic SST anomaly (*upper*) obtained from ocean reanalysis data, the corresponding principle component (PC) time series (*middle*), and the power spectral density of the PC. Significant levels are indicated by *long-dashed* (95 %) and *dotted* (90 %) *lines*. Contours are dimensionless. **b**, **c** Same as **a**, but for CTL and PDD runs, respectively. *Solid* and *dashed lines* in the PCA mode indicate the positive and negative values, respectively

decadal-to-interdecadal time scale, a 5–35 year bandpass filter was subsequently applied to all data. Consequently, a time scale longer than the decadal time scale remains. The same method was also applied to SST anomalies to depict air–sea coupled patterns. The lagged patterns shown in this study cover almost 8 years, which is about a quarter-to-half cycle of the decadal-to-interdecadal variations. As shown in Fig. 3, the sequential phase transition of SST anomalies from the negative to positive is clearly evident. A gradual southwestward migration of the negative SST anomaly is featured (Te Raa and Dijkstra 2002; Dijkstra 2006). Such migration resembles the "multidecadal SST mode". However, the stationary feature with a monopole pattern, the amplitude of which goes up and down with respect to time, is more dominant. The cold SST in the subpolar North Atlantic is associated with cyclonic atmospheric circulation in the middle atmosphere, of which the center is located at the southern tip of Greenland. Such a coherent pattern was also reported from an analysis of observed data (Wohlleben and Weaver 1995). After the cold SST anomaly moves to the southwest and then gradually weakens, it is replaced by a warm SST anomaly. At the same time, anticyclonic upper atmospheric circulation appears above the warm SST, and upper atmospheric circulation is subsequently intensified as the magnitude of the SST anomalies increases, indicating a strong air–sea interaction (Deser and Blackmon 1995; Kushnir 1994; Wohlleben and Weaver 1995). Basically, these features observed in the CTL run are very similar to those in the PDD run (not shown here) and thus, we omitted a description of the features in the PDD run.

In order to determine the dominant mechanism that induces the SST changes shown in Fig. 3, we analyzed the heat

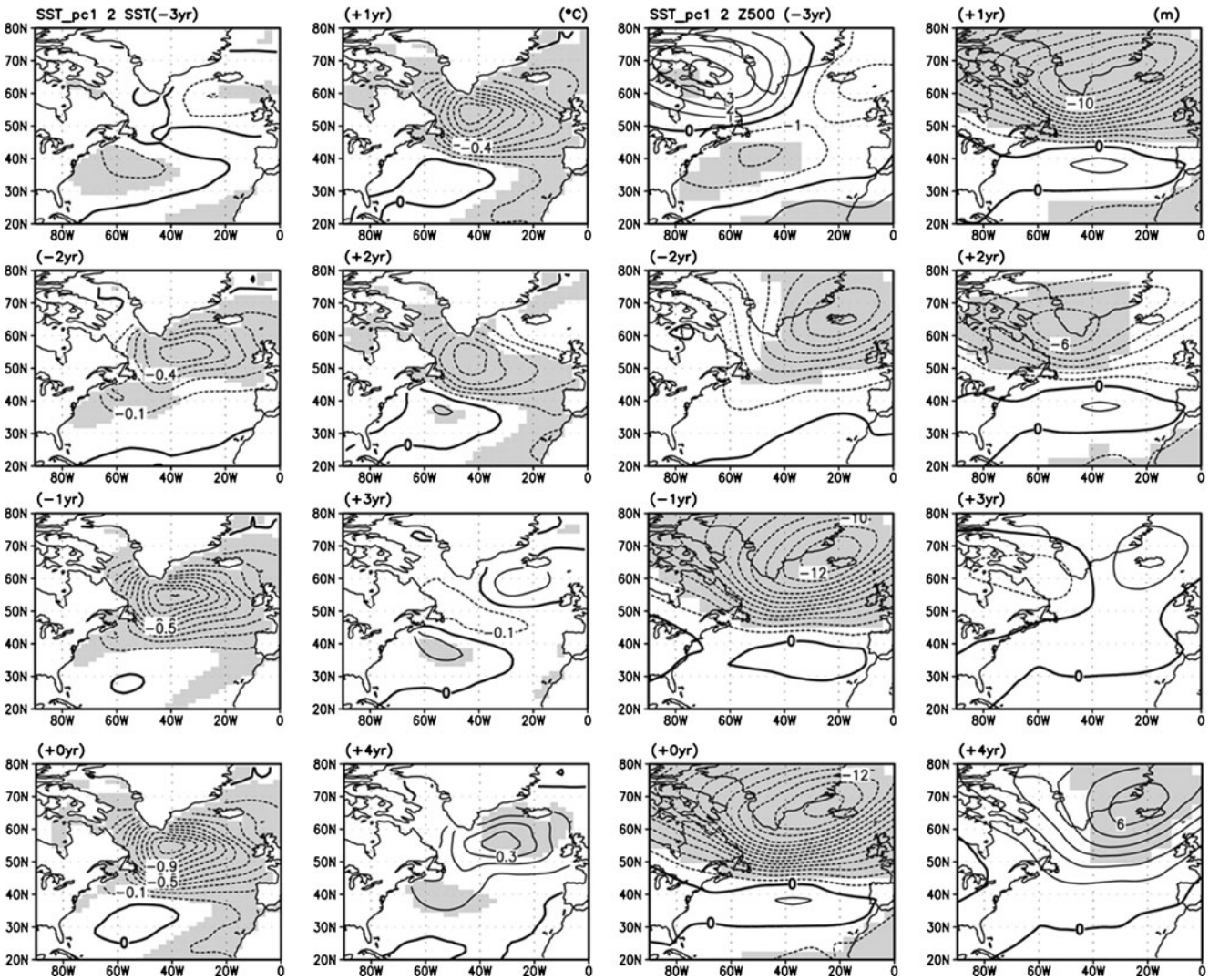

Fig. 3 Lagged linear regression map of the SST (left two columns) and 500 hPa geopotential height (right two columns) anomalies with respect to the first PCA PC time series of the North Atlantic SST anomaly obtained from the CTL run. Units for the SST and geopotential height are degree Celcius and meter, respectively. Statistically significant areas with 95 % confidence level are *shaded*. The 5–35 year bandpass filter is applied to all data

budget of the upper ocean heat content, which is defined as the vertical averaged ocean temperature from the surface to a depth of 200 m over 45–60°N. Since we are focusing on long-term fluctuations, a heat budget analysis of the upper ocean heat content is more reasonable than an examination of the SST because the upper ocean heat content naturally filters the short-term fluctuations that occur at the ocean surface. An area-averaged budget analysis is also applicable because the SST change in the North Atlantic is dominated by stationary features. The heat budgets include the net heat flux at the surface, as well as meridional and vertical thermal advections. Note that the vertical advection is smaller than the other terms by more than an order of magnitude and thus, it is neglected (not shown). The lead-lag regression of each term in the heat budget with respect to a change in the upper ocean heat content is shown in Fig. 4. The net heat flux, including the net short- and long-wave radiations, and the sensible and latent heat fluxes actually change with an upper ocean heat content change, which simultaneously acts as negative feedback. In contrast to the upper atmosphere trend, anticyclonic circulation at the surface over the subpolar Atlantic is associated with the cold SST (not shown here), which basically intensifies climatological surface atmospheric circulation over 45°–60°N, specifically the intensified westerly. Therefore, the intensified wind speed over 45°–60°N should lead to ocean surface cooling due to the enhanced release of latent heat, indicating positive feedback via "SST–wind–evaporation feedback". However, as shown in Fig. 4, the upper ocean heat content is negatively correlated to the net surface flux. Therefore, there must be another effect that overcompensates for this expected additional surface cooling.

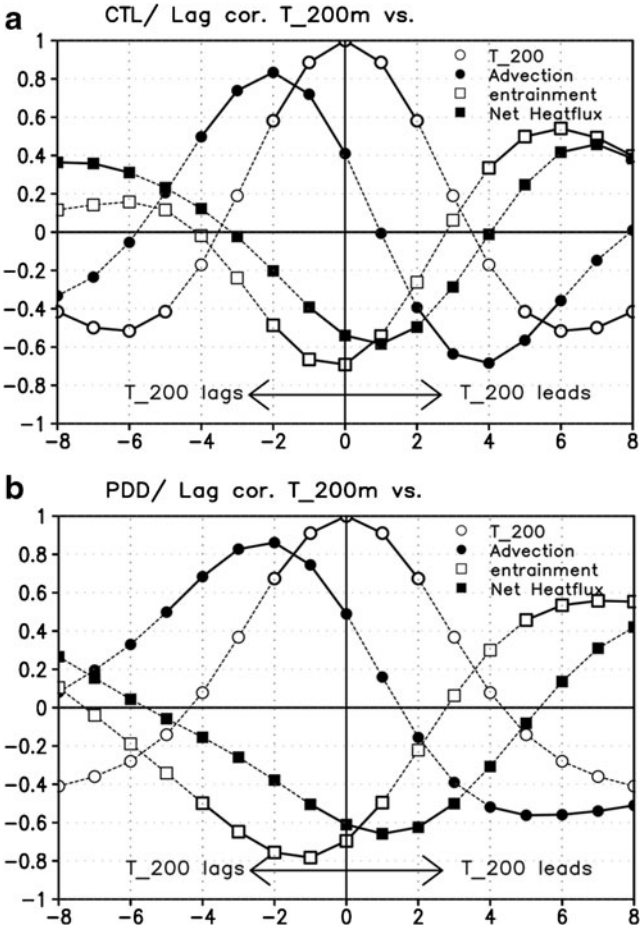

Fig. 4 **a** Lagged correlation of the North Atlantic heat content (*open circles*), meridional thermal advection (*closed circles*), entrainment (*open rectangles*), and surface net heat flux (*closed rectangles*) with respect to the North Atlantic heat content anomaly (temperature anomaly averaged horizontally over the 45–60°N latitudinal band and vertically over a depth of 0–200 m) obtained from the CTL run. Data are 5–35 year bandpass filtered. Negative (positive) lag means the ocean heat content is lagging (leading). **b** Same as **a**, but for the PDD run. *Solid lines* indicate the statistically significant with 90 % confidence level

On the other hand, cold (warm) meridional advection leads the cooling (warming) of the upper ocean heat content by about 2 years. Since the mean temperature decreases toward the north, the northward (southward) current accompanies warm (cold) advection. From Fig. 4, the expectation is that the strong southward current occurs around 2 years prior, while the strong northward current occurs around 4 years after the peak in upper ocean heat content cooling. Again, the southward current leads to the cooling by the cold advection and the northward current leads to the warming by the warm advection. To verify this feature, we computed the lagged regression of the zonally averaged zonal wind stress anomaly and zonally and vertically upper 200 m-averaged meridional current anomaly with respect to the first PCA PC time series of the North Atlantic SST anomaly obtained from both the PDD and CTL runs (see Fig. 2). As shown in Fig. 5, the evolution of the meridional current is consistent with that inferred from Fig. 4. That is, in the CTL run, the maximum southward current occurs 1–2 years before, which leads to the cooling, and the maximum northward current occurs 4 years after, which leads to the warming

If the meridional current that leads to the thermal advection is directly driven by the wind, like Ekman current, the wind stress change is more likely in-phase with the meridional current. This is because the time scale for the Ekman adjustment is shorter than 1 month. However, the wind stress curl by the zonal wind stress (not shown but the wind stress curl by the zonal wind stress is proportional to the meridional gradient of the zonal wind stress, $-\partial\tau^x/\partial y$) and the meridional current are not in-phase but time-lagged, inferring that the meridional current in this system is not dominated by the Ekman current (i.e., not directly wind driven). Furthermore, the meridional scale and location of the wind stress curl do not match those of the meridional current. The surface anticyclonic wind stress anomaly pattern (i.e., the negative wind stress curl) over the subpolar Atlantic, which is associated with the cold SST, is supposed to lead to a southward Sverdrup current. However,

as seen in Fig. 5, the northward current appears after the peak in the cold SST. Therefore, it can be inferred that the upper meridional current is not directly driven by the wind. This is related to the argument that the atmosphere drives the ocean over a shorter time scale; the opposite case is dominant for a longer time scale (Gulev et al. 2011).

Note that the positive wind stress curl anomaly over the Greenland–Iceland–Norwegian Sea was consistent with the negative SST anomaly over the subpolar North Atlantic in the CTL and PDD runs (not shown here). Thus, strengthening of the Greenland Sea gyre (Dickson et al. 1996) is supposed to lead to an intensification of the AMOC due to the introduction of a high salinity anomaly into the Greenland Sea gyre (i.e., negative feedback). However, this effect may not be critical in this model (see Figs. 5 and 8). Therefore, the role of wind stress in this model is rather passive with respect to oceanic changes over a longer time scale.

The results from both the CTL and PDD runs are basically similar, but the pattern from the CTL run shows more stationary features, while that for the PDD run exhibits a southward propagation feature. Overall, the phase transition and oscillatory features are more clearly depicted in the CTL run than in the PDD run. The phase transition in the PDD run seems to be delayed when compared to that in the CTL run.

As previously mentioned, the air–sea coupled pattern shown in Fig. 3 is very common, especially during the boreal winter. It is known that anticyclonic surface atmospheric circulation leads to the northward displacement of the Gulf Stream and a weakening of the Labrador Current. Consequently, northward heat transport by the Gulf Stream is enhanced, resulting in warming over the subpolar North Atlantic. Therefore, such an air–sea coupled process that occurs over the seasonal time scale operates as negative feedback. However, it is unclear whether or not the same mechanism also acts over the decadal-to-multidecadal time scale fluctuation.

4.2 Density driven

In the previous section, we demonstrated that thermal advection by the meridional current acts as prominent positive feedback, and the associated current is not directly driven by surface wind. Such results indicate that, over a long-term time scale fluctuation, the meridional current may rely more heavily on a change in the density rather than the wind. Here, we show the temporal evolution of the surface ocean density, which is represented by the lagged regression of the density anomaly with respect to the first PCA PC time series of the North Atlantic SST anomaly obtained from the CTL run. As shown in Fig. 6, a lower density appears over the ocean surrounding southern Greenland 3 years before the peak of the cold SST anomaly (−3 year lag) over the subpolar North Atlantic. In general, colder temperatures lead to a larger density. However, as the ocean temperature decreases (Fig. 3), the density anomaly also decreases, implying that the density is less influenced by temperature, but more dependent on the salinity. At zero lag, the density anomaly over the Labrador Sea becomes minimum, and a positive density anomaly begins to appear south of Iceland. This positive density anomaly gradually expands southwestward and, 4 years later, the phase of the density is completely changed when compared to the density anomaly 3 years before the peak of the cold temperature anomaly. The main feature in Fig. 6 is also observed in the PDD run (not shown here) and thus, we omit the description of the corresponding results. The differences between the CTL run and PDD run will be discussed later.

The meridional propagation features and the origin of the density anomaly were analyzed by computing the lagged regression of the zonal averaged density, salinity, and P–E against the PC time series of the first PCA of the SST obtained from the CTL run and PDD run. As shown in Fig. 7, the density anomaly propagates to the south at a speed of about 3.3°year^{-1}, and the salinity pattern matched the density pattern quite well. Such a result confirms that the density change is mainly dependent on the salinity change. As seen in Fig. 6, the density change leads to a temperature change by about 3–4 years, especially over the subpolar North Atlantic (55–70°N). However, around 50°N, the density and temperature anomalies are rather in-phase (upper panels of Fig. 7). In particular, the salinity change in the regression map is maximized at zero lag and 50°N. Such a result is attributed to the influence of the P–E. The P–E shows no propagation features and is simultaneously correlated to the PCs. Thus, the maximum regression of the P–E is observed at zero lag and 50–60°N, which matches the salinity change. The increase in the P–E mainly accounts for the decrease in evaporation due to the cold sea surface or the decrease in the saturated vapor pressure caused by the colder surface air temperature. The precipitation change does not significantly contribute to the change in the P–E. The main difference between the CTL run and PDD run in Fig. 7 is the relatively further delayed transition in the PDD run.

Finally, we calculate the regression map of the meridional overturning circulation (MOC, defined as the meridional stream function) over the North Atlantic with respect to the PC time series of the first PCA of the SST (Fig. 8). The mean MOC is positive over the North Atlantic, denoting clockwise rotation, i.e., a northward current in the upper ocean (less than 1,000 m in depth) and a southward current in the deep ocean (greater than 2,000 m in depth). The regression map of the MOC represents the negative anomaly through −3 to 1-year lags, indicating a slowing down of the MOC due to the reduced upper ocean density. The change in the upper ocean meridional current (see Fig. 5) is well correlated to that from the anomalous MOC, suggesting that the upper ocean meridional current is related to the MOC

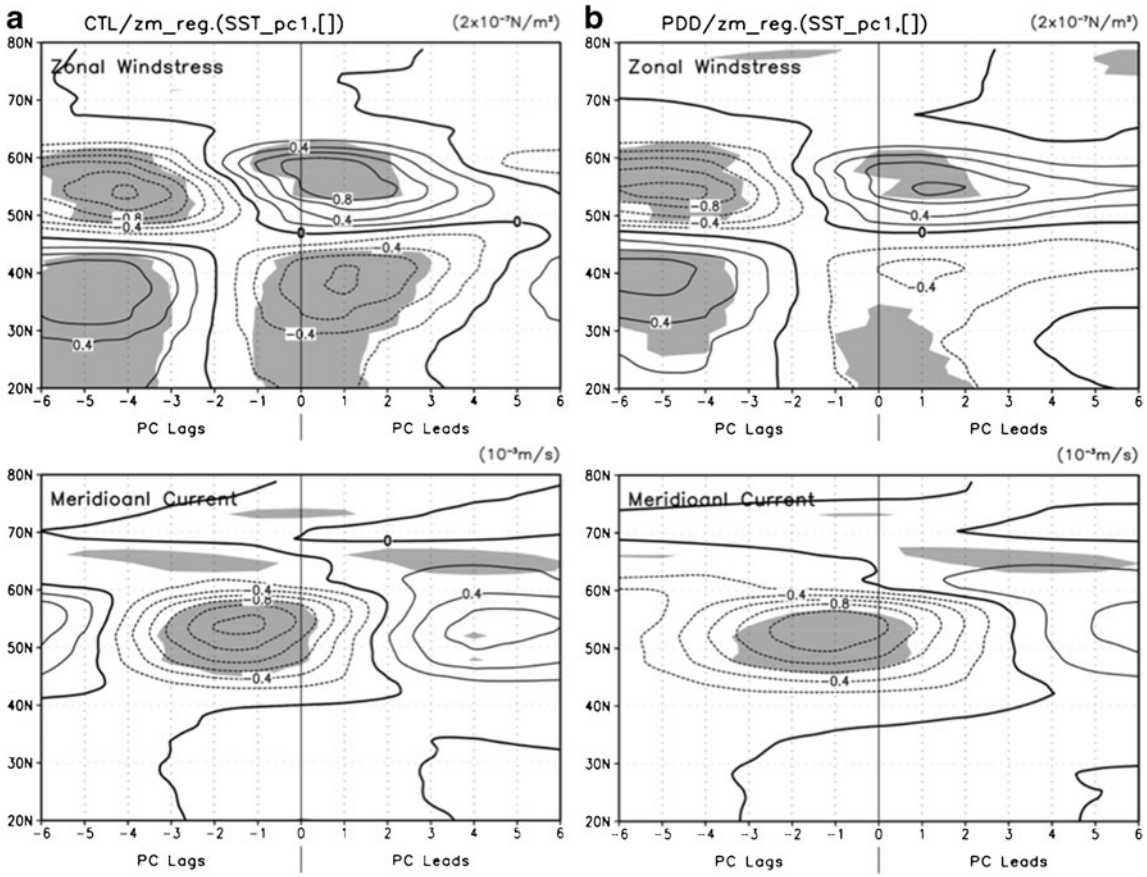

Fig. 5 **a** Lagged regression map of the zonally averaged wind stress anomaly (*upper left panel*) and zonally and vertically upper 200-m averaged meridional current anomaly (*lower left panel*) with respect to the first EOF PC time series of the North Atlantic SST anomaly obtained from the CTL run. **b** Same as **a**, but for the PDD run. Data are 5–35 year bandpass filtered. *Shading* indicates the statistically significant with 95 % confidence level

and driven by the density change. Note that a maximum anomalous MOC is observed at a −2 to −1 year lag and thus, the density change slightly leads the MOC change due to the delayed oceanic adjustment.

As mentioned above, the change in the MOC/meridional current is mainly caused by a change in density. Here, we propose that a change in the MOC/meridional current in turn leads to a change in the density. In order to complete an interdecadal oscillatory loop with a delayed negative feedback process, the above hypothesis was examined further. As seen in Fig. 6, the positive density anomaly starts to grow south of Iceland 1 year before the cold SST maximum. This positive density anomaly is related to density advection. Density advection by the meridional current influences the density anomaly, as represented in the following equation

$$\frac{\partial \rho'}{\partial t} \propto -\overline{v}\frac{\partial \rho'}{\partial y} - v'\frac{\partial \overline{\rho}}{\partial y}, \tag{3}$$

where a bar and prime denote the temporal mean and anomaly, respectively. When a negative density anomaly appears over the subpolar Atlantic (as in Fig. 6), both meridional advection of the anomalous density by the mean meridional current ($-\overline{v}\frac{\partial \rho'}{\partial y}$, where $\overline{v}$ is overall positive and $\frac{\partial \rho'}{\partial y}$ is negative) and meridional advection of the mean density by the anomalous meridional current ($-v'\frac{\partial \overline{\rho}}{\partial y}$, where $\frac{\partial \overline{\rho}}{\partial y}$ is positive and v' is negative in the case driven by density) become positive. Such a result may be attributed to a scenario where the negative density anomaly drives the negative meridional current anomaly due to suppression of the MOC (see Figs. 5 and 8). Therefore, the initial negative density anomaly over the subpolar Atlantic is reduced due to the positive tendency of the density anomaly associated with these two meridional density advection terms (see Fig. 11, which will be discussed in the next section). In particular, since $\frac{\partial \overline{\rho}}{\partial y}$ is largest over the south of Iceland (see Fig. 3 of Wang et al. 2010), the positive tendency of the density anomaly due to $-v'\frac{\partial \overline{\rho}}{\partial y}$ is largest. This positive density anomaly gradually expands to the west and grows so that the phase change occurs.

It was suggested that an anomalous high atmospheric pressure over Greenland enhances the flux of ice and freshwater through the Farm Strait into the Greenland

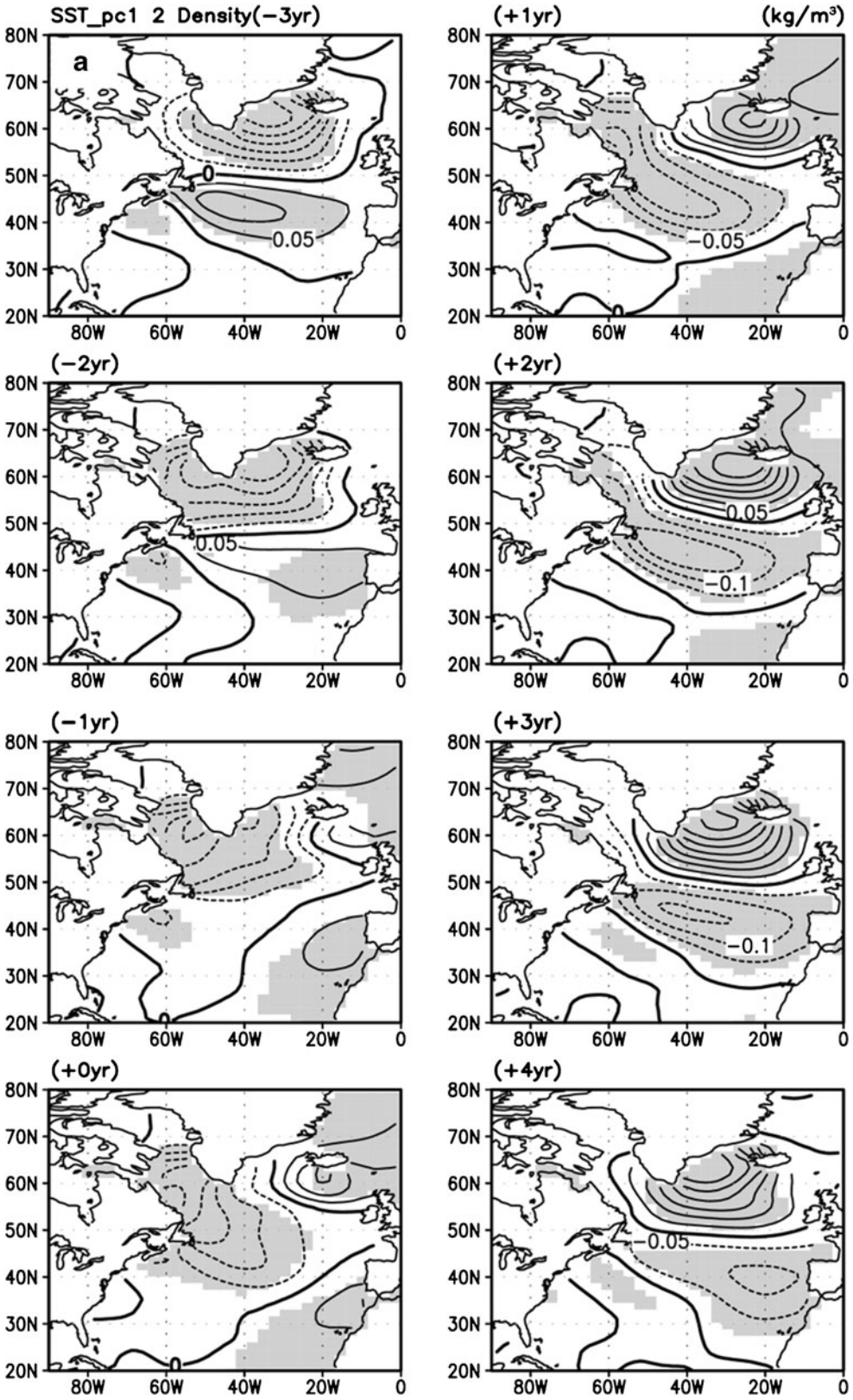

Fig. 6 Same as Fig. 3, but for the upper ocean density anomaly. Units are kilogram per cubic meter

Sea (Wohlleben and Weaver 1995). This flux ultimately enters the Labrador Sea and results in suppressed deep convection and AMOC due to the fresher surface water (Dickson et al. 1988; Mysak et al. 1990). In this regard, the higher sea level pressure anomaly over Greenland, which is associated with the cold SST over the subpolar

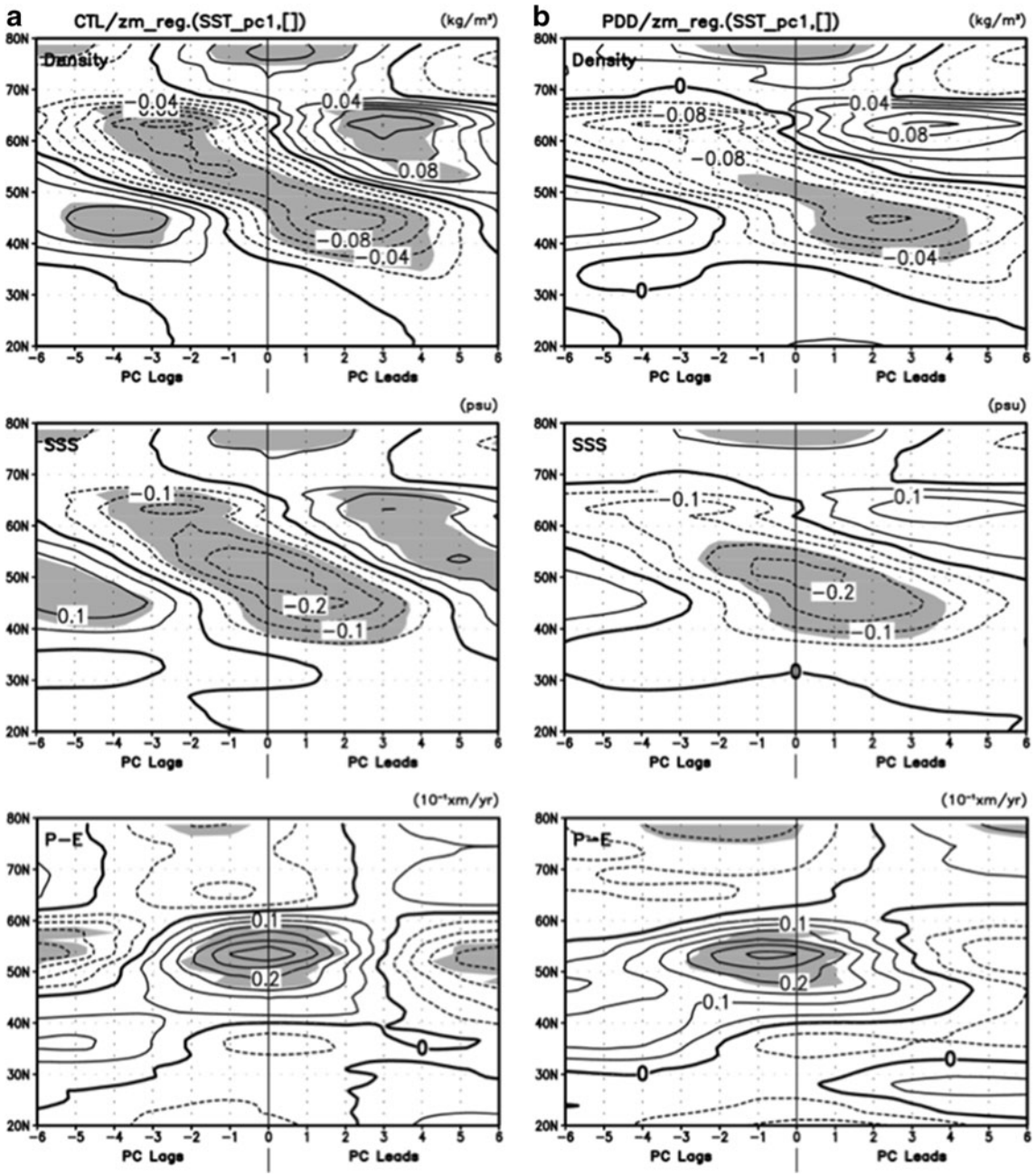

Fig. 7 **a** Same as Fig. 5, but for the upper ocean density (*upper panel*), salinity (*middle panel*), and P–E (*lower panel*) anomalies. P–E indicates the precipitation minus evaporation. **b** Same as **a** but for the PDD run

North Atlantic, is expected to suppress the MOC and thus, intensify ocean cooling due to reduced northward heat transport. Note that the sea level pressure anomaly is opposite to the 500 hPa geopotential height anomaly in Fig. 3 because of the baroclinic structure over the subpolar Atlantic in this long-term time scale. However, the oceanic resolution of FOAM is somewhat low and sea ice transport is not simulated in this model. Consequently, the intrusion of sea ice and fresh water through the Farm Strait is not easily realized

5 Role of Greenland ice sheet melting

In previous sections, a possible mechanism to drive an oscillatory loop of the North Atlantic long-term climate variability was proposed based on the lead/lag relationship between the density, MOC, and SST. Here, we investigate the role of Greenland ice sheet melting in this oscillatory loop. As shown in Fig. 9, the surface air temperature anomaly associated with the PC time series of the first PCA of the SST anomaly obtained from the CTL run shows that the

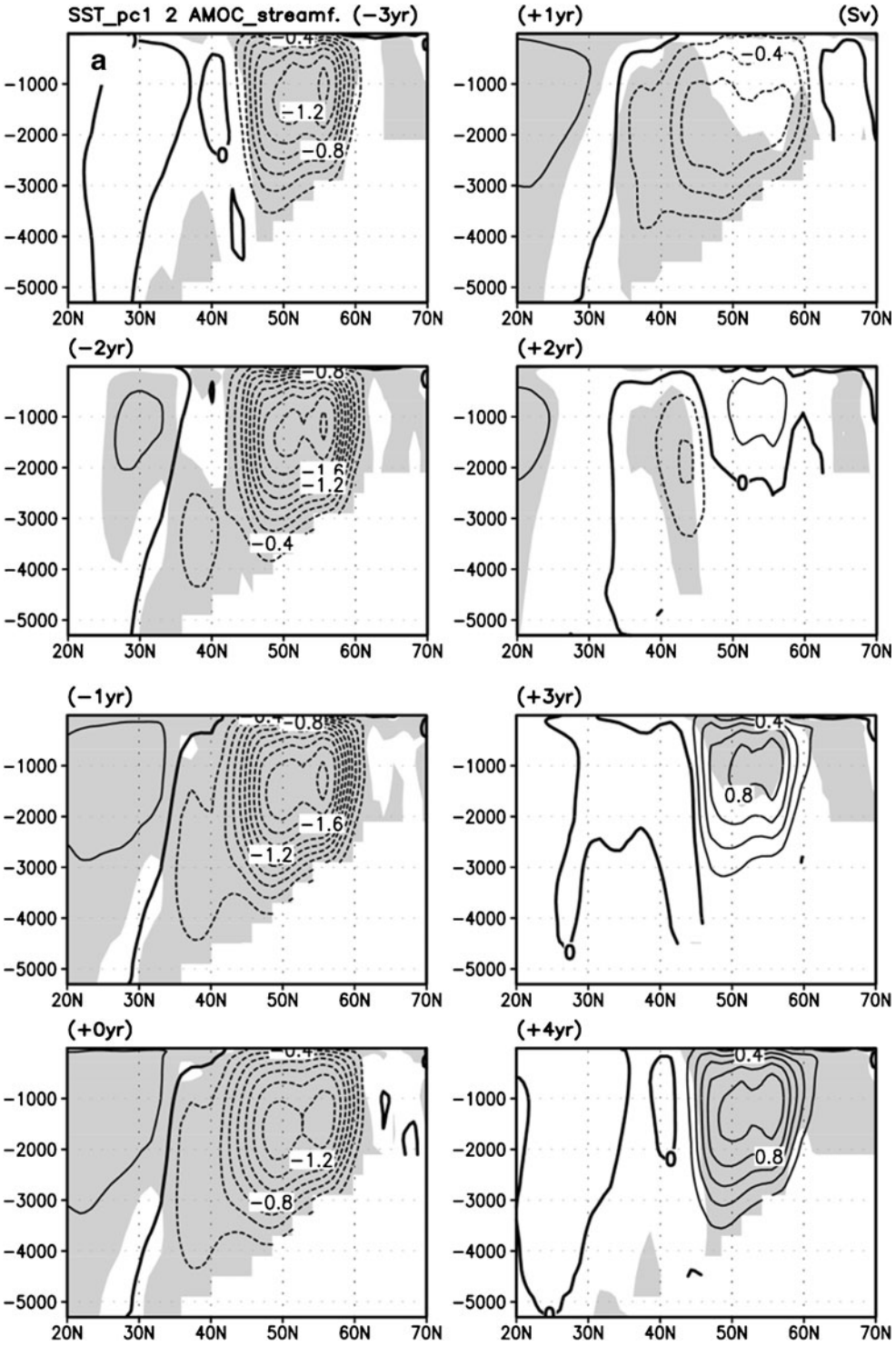

Fig. 8 Same as Fig. 3, but for the oceanic meridional stream function anomaly obtained from the CTL run. Units are sverdrups [$(100\ \mathrm{m})^3\,\mathrm{s}^{-1}$]

evolution and amplitude changes in the surface air temperature anomaly closely match those of the SST anomaly in Fig. 3. This implies that the SST regulates the surface air temperature, especially over the longer time scale, but not the other way around. In other words, the negative SST anomaly leads to the negative surface air temperature anomaly, and the cold surface air temperature reduce the melting of ice and consequently the freshwater discharge is reduced, which results in an increase in the ocean density and an enhancement in the MOC.

As can be seen in Fig. 10, the mean runoff in the PDD run (0.043 Sv for the last 200-year mean) is larger than that in the CTL run (0.032 Sv for the last 200-year mean). Such an increase is attributed to the lower salinity, as seen in Fig. 1b.

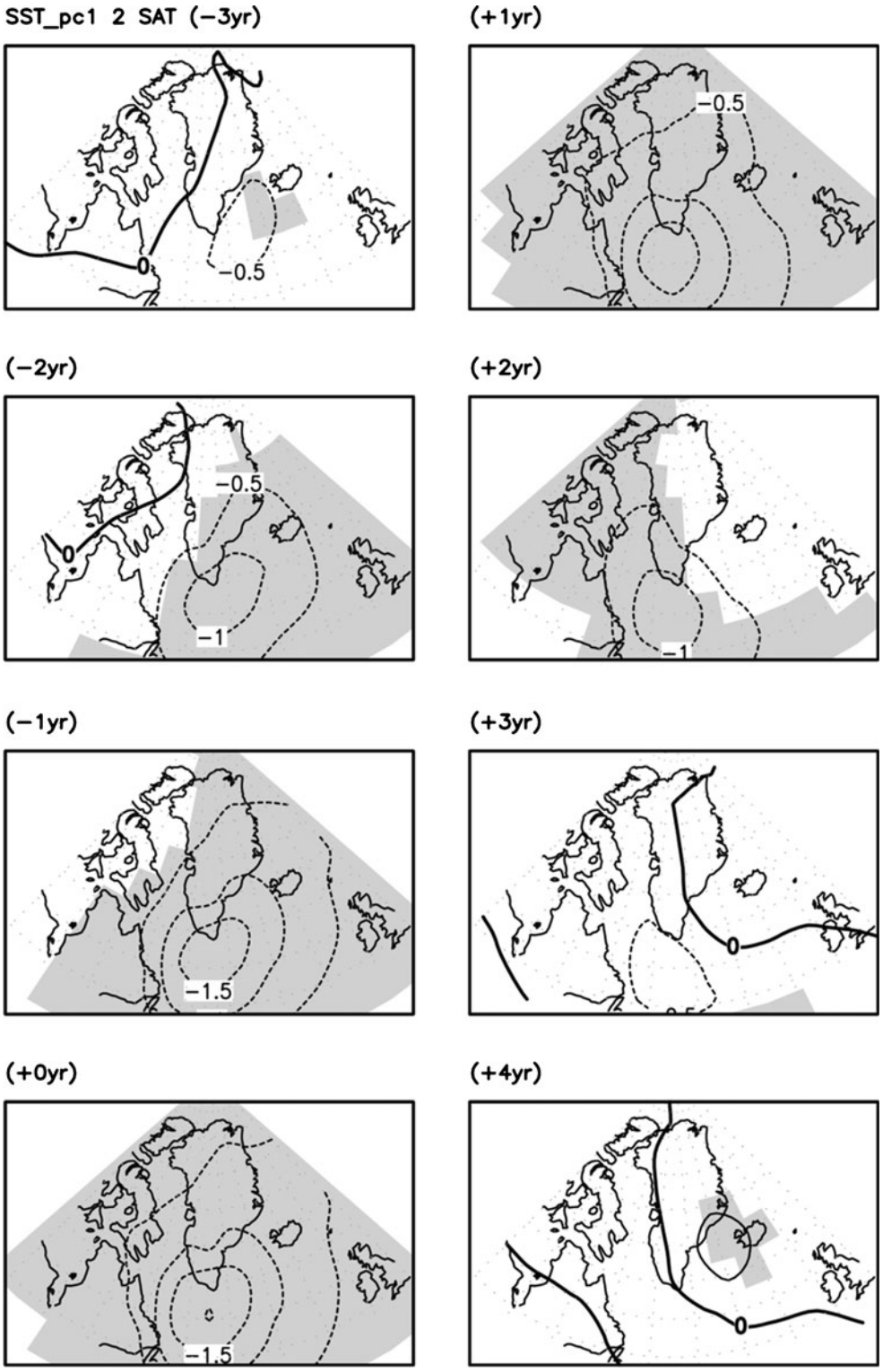

Fig. 9 Same as Fig. 3, but for the surface air temperature anomaly and PDD run

The variance of the runoff in the PDD run is also larger than that in the CTL run. The runoff and P–E over the North Atlantic are negatively correlated with correlation coefficients of −0.38 (CTL run) and −0.48 (PDD run), which are statistically significant with 99 % confidence levels. This is because the cold SST anomaly results in an increase of the P–E, but a decrease in ice melting. This negative feedback operates in the PDD run, but not in the CTL run.

Another possible impact of Greenland ice sheet melting is related to the change in the mean state. The mean state change shown in Fig. 1 can modify the feedback process. As mentioned in the previous section, meridional density

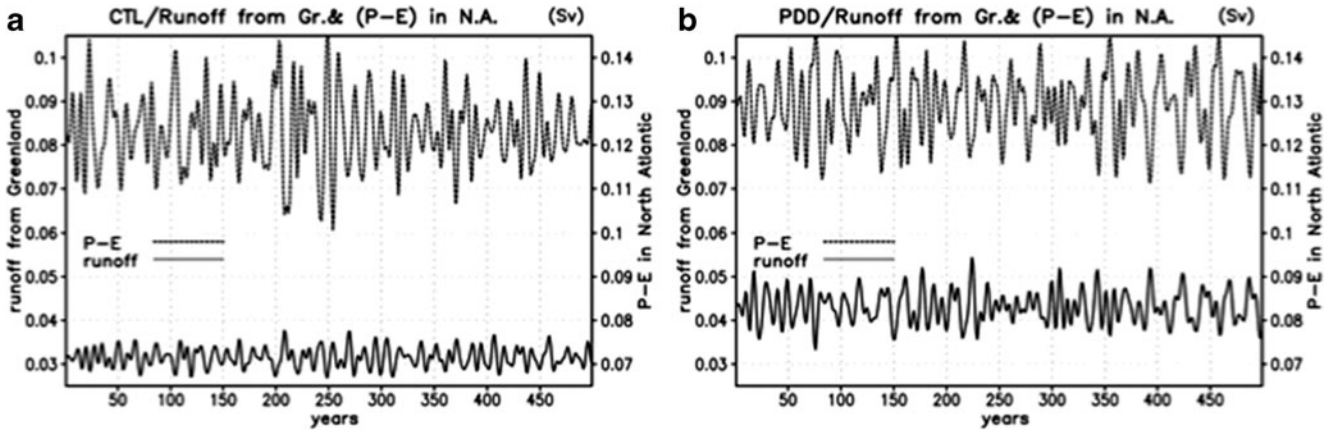

Fig. 10 River runoff from Greenland (*solid line*, scales on the left) and P–E over the North Atlantic (*dashed line* scales on the right), as obtained from **a** the CTL run and **b** the PDD run (*dashed line*). Units are sverdrups. The time mean of P–E for CTL run and PDD run are 0.123 and 0.129 Sv, respectively, and the time mean of runoff for CTL run and PDD run are 0.0315 and 0.0431 Sv, respectively

advection plays an important role in the phase transition in the oscillatory loop by acting as negative feedback. This negative feedback is modified in a changing climate state associated with Greenland ice sheet melting. As seen in Fig. 1, both the mean meridional current and the meridional gradient of the mean density of the PDD run are relatively small when compared to those in the CTL run (i.e., $0 < \overline{v}_{\mathrm{PDD}} < \overline{v}_{\mathrm{CTL}}$ and $0 < (\partial\overline{\rho}/\partial y)_{\mathrm{PDD}} < (\partial\overline{\rho}/\partial y)_{\mathrm{CTL}}$). Thus, the density tendency due to both $-\overline{v}\frac{\partial\rho'}{\partial y}$ and $-v'\frac{\partial\overline{\rho}}{\partial y}$ in the PDD run is expected to be smaller than that in the CTL run. Consequently, the negative feedback due to these density advections is expected to be weaker in the PDD run than in the CTL run. To confirm this argument, we computed the lagged regressions of two meridional density advections with respect to the ocean density (Fig. 11). In this calculation, all quantities have been volume-averaged horizontally over the 45–60°N latitudinal band and vertically over a depth of 0–200 m. In the CTL run, $-v'\frac{\partial\overline{\rho}}{\partial y}$ strongly influences the density change as negative feedback (as mentioned above), while the impact of $-\overline{v}\frac{\partial\rho'}{\partial y}$ is relatively small. However, in the PDD run, the negative feedback due to $-v'\frac{\partial\overline{\rho}}{\partial y}$ becomes significantly reduced when compared to that in the CTL run, while $-\overline{v}\frac{\partial\rho'}{\partial y}$ somewhat influences the ocean density as positive feedback. Therefore, a slow transition and longer time scale fluctuation in the PDD run is attributed to a reduction in such slightly lagged negative feedback associated with these two density advections.

In summary, local air–sea–ice interactions increase negative feedback, while the mean state change induced by Greenland ice sheet melting suppresses negative feedback. While a quantitative comparison of these two opposite effects may not be easy, we could argue that, when compared to the CTL run, the slower phase shift and lower frequency oscillation in the PDD run are likely due to the fact that the suppression of negative feedback associated with a change in the mean state overcompensates for additional negative feedback due to local air–sea–ice interactions.

6 Summary and discussion

In this study, we investigated the role of Greenland ice sheet melting on climate variability over the North Atlantic. The ice sheet melting rate was calculated via the PDD method, which was incorporated into a coupled ocean-atmosphere model, FOAM. Greenland ice sheet melting resulted in an increase in climatological–mean freshwater discharge, which leads to sea surface cooling over the Labrador Sea due to the suppression of the North Atlantic meridional overturning circulation. Reduced ocean surface evaporation due to a colder ocean surface contributed to a further reduction in the surface ocean density.

Models both with and without the PDD method produced a realistic pattern of North Atlantic SST variability that fluctuated from decadal to interdecadal periods. However, significant longer interdecadal variability was only observed in the PDD run. The quasi-oscillatory mode is mainly driven by feedback processes related to density. This oscillatory loop may be described as follows. The lower surface density suppresses the AMOC and weakens northward heat transport, which leads to a decrease in the ocean surface temperature over the subpolar North Atlantic by 3–4 year lags. The cold ocean surface reduces surface evaporation and thus, the ocean surface becomes fresher and the AMOC is further reduced, namely acting as positive feedback. On the other hand, density advection by the southward anomalous meridional current leads to a positive tendency of the density anomaly, which is opposite to the initial negative density anomaly. This negative feedback acts as a transition mechanism. Anticyclonic surface atmospheric circulation over

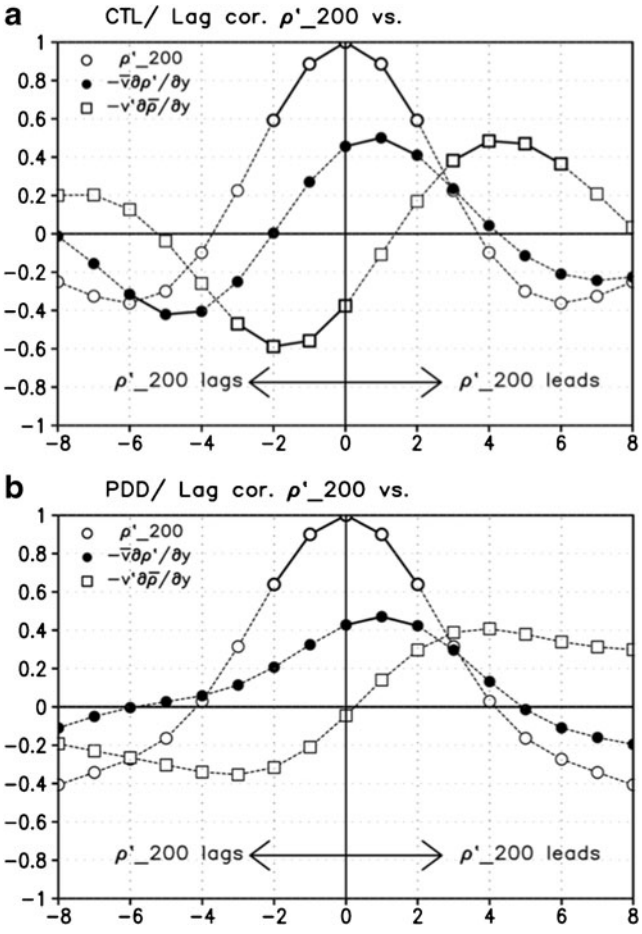

Fig. 11 **a** Lagged regression of the North Atlantic density (*closed circles*), anomalous density advection by the mean meridional current (*open circles*), and mean density advection by the anomalous meridional current (*open rectangular*) with respect to the North Atlantic density anomaly (averaged horizontally over the 45–60°N latitudinal band and vertically over a depth of 0–200 m) obtained from the CTL run. Negative (positive) lag means the ocean density is lagging (leading). **b** Same as **a**, but for the PDD run. For easy interpretation, the signs for all curves are reversed. *Solid lines* indicate the statistically significant with 90 % confidence level

the cold SST region influences the ocean current, but does not play a dominant role in longer time scale variations. Finally, when the Greenland ice melting process is incorporated in the system, the cold (warm) SST acts to decrease (increase) the ice melting rate, which intensifies (reduces) the AMOC and warm (cold) advection. Therefore, the melting of the Greenland ice sheet works as negative feedback. However, the melting of the ice sheet also modifies the climate state over the subpolar Atlantic, which actually acts to reduce the negative feedback associated with density advection by the meridional current. The former is actually overcompensated by the latter and thus, the reduced negative feedback causes the low frequency and slow transition of the quasi-oscillatory mode in the PDD run. This oscillatory mode may not be self-sustained, but rather damped so that the stochastic forcing that supplies the energy and triggers the mode is necessary.

It is known that long-term climate variability in the subpolar North Atlantic is driven by complicated air-sea-ice feedback loops (Grossmann and Klotzbach 2009). In contrast to other studies (Wu and Liu 2005; Alvarez-Garcia et al. 2008), this work emphasizes the role of salinity-driven flow (Frankcombe and Dijkstra 2010), where the salinity change depends on density advection by current, air-sea interactions, and freshwater discharge due to Greenland ice sheet melting. Using the FOAM, Wu and Liu (2005) demonstrated that North Atlantic climate variability is composed of monopole and tripole modes that are dominated by decadal-to-multidecadal and interannual-to-decadal variabilities, respectively. They especially focused on the tripole mode, which is driven via positive feedback associated with coupling between the North Atlantic Oscillation and the SST tripole pattern, as well as delayed negative feedback associated with the adjustment of the subtropical gyre in response to an associated wind stress curl. On the other hand, we focused on the decadal-to-interdecadal monopole mode, which is mainly driven by density-related feedback processes. It should be noted that in the work of Wu and Liu (2005), the first and second EOF modes of the observed SST anomaly were monopole and tripole modes, respectively. This order was switched in the FOAM-simulated SST anomaly. In our calculations, the first EOF mode exhibited a monopole pattern (Fig. 2). This discrepancy between our study and the work of Wu and Liu (2005) is mainly attributed to a difference in the averaging method; we employed the annual average, while Wu and Liu (2005) used the winter average (DJF), which had been checked by computing the EOF mode of the DJF-averaged SST anomaly.

Acknowledgments The authors thank Profs. A. Timmermann and H. Yang for their valuable comments. This work was supported by SBS foundation and the Polar Academic Program (PAP), KOPRI.

References

Abdalati W, Steffen K (2001) Greenland ice sheet melt extent: 1979–1999. J Geophys Res 106:33,983–33,988

ACIA (2005) Arctic climate impacts assessment. Cambridge University Press, New York, p 1042

Alvarez-Garcia F, Latif M, Biastoch A (2008) On multidecadal and quasi-decadal North Atlantic variability. J Climate 21:3433–3452

Braithwaite RJ (1995) Positive degree-day factors for ablation on the Greenland ice sheet studied by energy-balance modelling. J Glaciol 41:153–159

Braithwaite R, Olesen OB (1989) Calculation of glacier ablation from air temperature, west Greenland. In: Oerlemans J (ed) Glacier fluctuations and climatic change. Kluwer, Dordrecht, pp 219–233

Bryden HL, Longworth HR, Cunningham SA (2005) Slowing of the Atlantic meridional overturning circulation at 25° N. Nature 438:655–657

Chen JL, Wilson CR, Tapley BD (2006) Satellite gravity measurements confirm accelerated melting of Greenland ice sheet. Science 313:1958–1960

Deser C, Blackmon ML (1995) Surface climate variations over the North Atlantic Ocean during winter: 1900–1989. J Clim 6:1743–1753

Deser C, Phillips AS, Alexander MA (2010) Twentieth century tropical sea surface temperature trends revisited. Geophys Res Lett 37: L10701. doi:10.1029/2010GL043321

Dickson RR, Brown J (1994) The production of North Atlantic deep water: sources, rates and pathways. J Geophys Res 99:12319–12341

Dickson RR, Meincke J, Malmberg S-A, Lee AJ (1988) The "Great Salinity Anomaly" in the northern North Atlantic 1968–1982. Prog Oceanogr 20:103–151

Dickson RR, Lazier J, Meincke J, Rhines P, Swift J (1996) Long-term coordinated changes in the convective activity of the North Atlantic. Prog Oceanogr 38:241–295

Dijkstra HA (2006) Interaction of SST modes in the North Atlantic Ocean. J Phys Oceanogr 36:286–299

Eden C, Jung T (2001) North Atlantic interdecadal variability: oceanic response to the North Atlantic oscillation (1865–1997). J Climate 14:676–691

Frankcombe LM, Dijkstra HA (2010) Internal modes of multidecadal variability in the Arctic Ocean. J Phys Oceanogr 40:2496–2510

Grossmann I, Klotzbach PJ (2009) A review of North Atlantic modes of natural variability and their driving mechanisms. J Geophys Res 114:D24107. doi:10.1029/2009JD012728

Gulev S, Latif M, Keenlyside N (2011) Reconstruction of observationally-based 130-year (1880–2010) time series of surface turbulent fluxes in the North Atlantic: prospects for studying North Atlantic climate variability on decadal to centennial time scales. Proceedings of WCRP OSC 2011 Meeting

Hock R (2003) Temperature index melt modelling in mountain areas. J Hydrol 282:104–115

Holland MM, Bitz CM (2003) Polar amplification of climate change in the Coupled Model Intercomparison Project. Clim Dyn 21:221–232

IPCC (2007) In: Solomon S, Qin D, Manning M, Chen Z, Marquis M, Averyt KB, Tignor M, Miller HL (eds) Climate change 2007: the physical science basis. Contribution of Working Group I to the Fourth Assessment Report of the Intergovernmental Panel on Climate Change. Cambridge University Press, Cambridge

Jacob RL (2007) Low frequency variability in a simulated atmosphere ocean system. Ph. D. Thesis. Univ of Wisconsin Madison. pp. 172

Kushnir Y (1994) Interdecadal variations in North Atlantic sea surface temperature and associated atmospheric conditions. J Clim 7:141–157

Liu Z, Kutzbach J, Wu L (2000) Modeling climate shift of El Nino variability in the Holocene. Geophys Res Lett 27:2265–2268

Lozier MS, Roussenov V, Reed MSC, Williams RG (2010) Opposing decadal changes for the North Atlantic meridional overturning circulation. Nat Geo 3:728–734

Marshall J, Schott F (1999) Open-ocean convection: observations, theory and models. Rev Geophys 37:1–64

Rothrock DA, Percival DB, Wensnahan M (2008) The decline in arctic sea-ice thickness: separating the spatial, annual, and interannual variability in a quarter century of submarine data. J Geophys Res 113:C05003. doi:10.1029/2007JC004252

Schlesinger ME, Ramankutty N (1994) An oscillation in the global climate system of period 65–70 years. Nature 367:723–726

Serreze MC et al (2003) A record minimum arctic sea ice extent and area in 2002. Geophys Res Lett 30. doi:10.1029/2002GL016406

Smith TM et al (2008) Improvements to NOAA's historical merged land–ocean surface temperature analysis (1880–2006). J Clim 21:2283–2296

Te Raa LA, Dijkstra HA (2002) Instability of the thermohaline ocean circulation on interdecadal timescales. J Phys Oceanogr 32:138–160

Ting M, Kushnir Y, Seager R, Li C (2009) Forced and internal twentieth-century SST trends in the North Atlantic. J Climate 22:1469–1481

Wang C, Dong S, Munoz E (2010) Seawater density variations in the North Atlantic and the Atlantic meridional overturning circulation. Clim Dyn 34:953–968

Wohlleben TM, Weaver AJ (1995) Interdecadal climate variability in the subpolar North Atlantic. Clim Dyn 11:459–467

Wu L, Liu Z (2002) Is tropical Atlantic variability driven by the North Atlantic oscillation? Geophys Res Lett 29. doi:10.1029/2002GL014939

Wu L, Liu Z (2005) North Atlantic decadal variability: air–sea coupling, oceanic memory, and potential northern hemisphere resonance. J Clim 18:331–349

Wu L, Liu Z, Gallimore R, Jacob R, Lee D, Zhong Y (2003) Pacific decadal variability: the tropical Pacific mode and the North Pacific mode. J Climate 16:1101–1120